SEMARAK ILMU PUBLISHING

CFD Letters

Journal homepage:
https://semarakilmu.com.my/journals/index.php/CFD_Letters/index
ISSN: 2180-1363

Computational Investigation into Prediction of Lift Force and Resistance of a Hydrofoil Ship

Ahmad Fitriadhy[1,*], Intan Nur Nabila[1], Christina Bangi Grosnin[1], Faisal Mahmuddin[2], Suandar Baso[3]

[1] Programme of Naval Architecture, Faculty Ocean Engineering Technology and Informatics, Universiti Malaysia Terengganu, Malaysia
[2] Department of Marine Engineering, Engineering Faculty, Hasanuddin University Jalan Perinits Kemerdekaan km. 10, Tamalanrea, Makassar, Indonesia
[3] Department of Naval Architecture, Faculty of Engineering, Hasanuddin University, Jalan Poros Malino, KM. 6 Bontomarannu, 92172, Gowa, Sulawesi Selatan, Indonesia

ARTICLE INFO

Article history:
Received 24 March 2022
Received in revised form 20 April 2022
Accepted 21 April 2022
Available online 30 April 2022

Keywords:
Computational fluid dynamics (CFD); coal-fired utility boiler; ash deposition; combustion; ash sampling

ABSTRACT

The characteristics of the fore and aft foils at the various angles of attack incorporated with forward velocities have been vulnerable to induce strong nonlinearities to dynamic lift force and ship resistance. Then, a computational simulation is necessarily required to predict their performances in the calm water condition. This paper presents a computational investigation of the hydrofoil ship on predicting lift and ship's resistance using fluid dynamic (CFD) simulation approach. Several parameters such as Froude numbers and the angle of attacks both of fore and aft foils have been accordingly taken into account. The results revealed that the subsequent increase on angle of attack of fore and aft foils was directly proportional to the lift force and the ship's resistance. In addition, the lift force of the aft and fore foils with the angle of attacks of 10 degrees and 5 degrees, respectively, resulted in the significant increase of the lift force and the ship's resistance. However, the subsequent increase of Froude number from 1.382 up to 1.626 has insignificant effect to the lift and the ship's resistance of the hydrofoil. It can be concluded that CFD simulation is very beneficial to ensure an operational effectiveness of hydrofoil design towards prediction on the lift force and the hydrofoil's resistance at the preliminary design stage.

1. Introduction

The use of hydrofoil on a boat is specially aimed to reduce the viscous resistance of the boat while moving in the water. The utilization of the hydrofoil has their own advantages and disadvantages in marine design industry [1]. One of the disadvantages is that the vibration of the foil structure leads to fatigues of the system [2]. However, the hydrofoil or known as lifting foil [3] is able to produce sufficient lifting force at relatively high speed. Inherently, the hull can be lifted out of the water as well as the ship's wetted surface area (WSA), where the ship's resistance reduces [4]. In other words, the ship's displacement reduces due to presence of the lift force arisen the boat [5]. Geometrically, the hydrofoils are installed under the hull of the ship and have moved underwater, near the free

* *Corresponding author.*
E-mail address: a.fitriadhy@umt.edu.my (Ahmad Fitriadhy)

https://doi.org/10.37934/cfdl.14.4.5166

surface of the water. As a result, the waves generated by the movement of the ship may have an impact on the hydrofoil performance and the revenue of the ship [6]. The technology of hydrofoil is undergoing a re-mergence, where the hydrofoils technology has become more reliable and widely used for fast commercial ferries.

Numerous geometrical studies have been conducted by the researches on the prediction of ship's resistance through analytical, numerical and experimental approaches towards achieving lower total ship's resistance. According to the study by Besana & Turnock [7], L-fois, C-foils, horizontal foils are the example shapes of a hydrofoil which are attached to the hull of a boat in different configurations. Two general hydrofoil configurations that have been used historically, commercially, and experimentally is the surface piercing foil and the fully submerged foil [8]. Based on research done by Putranto & Sulisetyono [5], the displacement of ship incorporated with the hydrofoil will decrease because the lift force will support the ship upraised. It should be noted here that the characteristics of the fore and aft foils at the various angles of attack incorporated with forward velocities have been vulnerable to induce strong nonlinearities to dynamic lift force and ship resistance. This occurs since the presence of the hydrofoil affects significant increase of the added ship's resistance. The phenomenon may be possibly happening where the ship will experience higher resistance compared to a ship without hydrofoil ones in the low forward speed and vice-versa. Therefore, the effective design, durable and affordable hydrofoil systems need to be developed and comprehensively analyzed (Figure 1) [9]. The experimental model study on the hydrofoil lifting force prediction at the towing has been prone to cost; whilst theoretical approach may lead to less accuracy of the result. Hence, the investigation on the hydrofoil using computational fluid dynamic approach is necessarily required to obtain more reliable prediction on lifting force and ship's resistance.

This paper presents Computational Fluid Dynamic (CFD) simulation into prediction of lift force and ship's resistance of a hydrofoil in the calm water condition. Several parameters such as the effect of the various fore and aft hydrofoil angles of attack and Froude numbers, have been accordingly taken into consideration in computational simulation. The angles of attack for the fore and aft hydrofoils are 0, 5, 10, and 15 degrees incorporated with the various forward velocities. Here, the commercial software called Fine™/Marine simulation has been utilized to predict her lift force and the total ship's resistance. Finally, the CFView™/Marine is then used to visualize the hydrodynamic performance around the hydrofoil. The results of the lift force and the ship's resistance characteristics of the hydrofoil ship using the CFD approach are then accordingly discussed in Section 3.

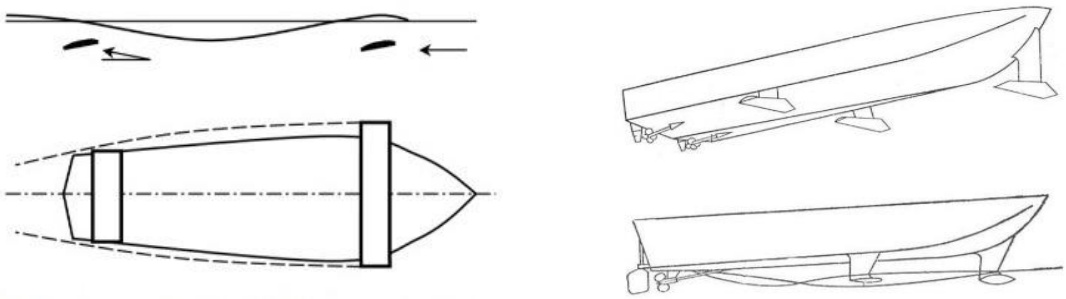

Fig. 1. A hydrofoil craft concept [9]

2. Methodology

2.1 Conservation Equation

CFD analysis entails numerically solving the governing equations of fluid flow. There are three governing equations of fluid flow [10].

The mass conservation for incompressible flow is shown as in Eq. (1)

$$\frac{\partial(\mathrm{u})}{\partial \mathrm{x}}+\frac{\partial(\mathrm{v})}{\partial \mathrm{y}}+\frac{\partial(\mathrm{w})}{\partial \mathrm{z}}=0 \tag{1}$$

where u, v, and w are the fluid velocities in the x, y, and z directions, respectively.

Continuity and Navier-Stokes equations are used to represent the motion of viscous fluid. This equation is derived from the law of conservation of momentum [11]. The continuity and Navier-Stokes equations are given as follows

$$\frac{\partial u_i}{\partial x_i}=0 \tag{2}$$

$$\frac{\partial u_i}{\partial t}+u_j\frac{\partial u_t}{\partial x_j}=f_i-\frac{1}{\rho}\frac{\partial p}{\partial x_i}+\frac{1}{\rho}\frac{\partial \tau_y}{\partial x_j} \tag{3}$$

where ρ is the density, u_i is the velocity vector, f_i are body forces per unit mass, p is the pressure while τ_y is the viscous stress tensor which is defined as below

$$\tau_y=\mu(\frac{\partial u_i}{\partial x_j}+\frac{\partial u_j}{\partial x_i} \tag{4}$$

where μ is the dynamic viscosity.

2.2 k-ω Turbulence Model

The k-omega turbulence model is used where k is the turbulent kinetic energy and ω is the specific dissipation rate. The k-omega model is set to improve the predictions obtained with algebraic mixing-length models in order to achieve a local model for complex flows. The two major features of this model are the zonal blending of model coefficients and limitations on the growth of the eddy viscosity in rapidly strained flows [12]. Besides that, it also displays a simpler alternative to two-equation turbulence model, for example the k-epsilon model [13].
The model coefficients are written as

$$\frac{\partial \rho K}{\partial t}+\frac{\partial}{\partial x_i}(\rho U_j K-(\mu+\sigma_k\mu_i)\frac{\partial K}{\partial x_i}=\tau_{ij}S_{ij}-\beta^*\rho\omega K \tag{5}$$

$$\frac{\partial \rho\omega}{\partial t}+\frac{\partial}{\partial x_j}\left(\rho U_j\omega-\mu+\sigma_\omega\mu_t\right)\frac{\partial \omega}{\partial x_j}=P_\omega-\beta\rho\omega^2+2(1-F^1)\frac{\rho\sigma_{\omega 2}}{\omega}\frac{\partial K}{\partial x_j}\frac{\partial \omega}{dx_j} \tag{6}$$

Eq. (6) is the cross-diffusion term that is in the transformed omega-equation from the epsilon-equation.

The k-epsilon model is commonly used in marine CFD industry for resistance calculation and yield nearly identical result to the k-omega for favorable pressure gradients with little or no flow

separation. Resistance offered by ship movement through water resolved into two principal components: frictional resistance and residual resistance [14]. However, use of the RNG model has not generally led to my significant improvement. The better performances in heave and pitch may result in lower added resistance in waves [15]. Heave is an oscillatory linear motion of the vessel in the direction of its vertical axis, is taken into account mainly because it has a tendency to be more closely coupled with the pitch mode [16].

2.3 Main Dimensions

The 3D model of the hydrofoil ship is clearly displayed in Figure 2. This hydrofoil ship has two foils i.e., aft and fore foils, which are designed using the NACA Model series of 0015. These hydrofoils mainly provide sufficient lift force to lift the boat's hull outside the water [17]. The principal dimension of the hydrofoil ship is summarized in Table 1.

Table 1
Principal dimension of hydrofoil ship

Description	Full scale	Model scale
Length Overall, LOA (m)	32.64	16.32
Length Between Perpendicular, LBP (m)	32.276	16.138
Beam, B (m)	8.278	4.139
Draft, T (m)	1.4	0.7

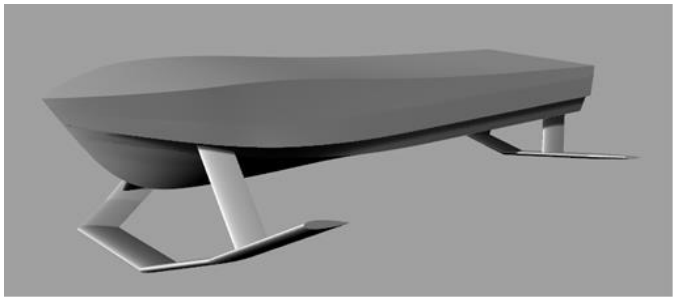

Fig. 2. 3D model of hydrofoil ship

2.4 Simulation Condition

Following the CFD application on the naval architecture fields [18-25], the computational simulations have been extended to predict the lift force and the ship's resistance of the hydrofoil ship in the calm water condition. Several parameters such as the various angles of attacks for the fore and aft foils and the effects of the Froude numbers are taken into the computational simulations. Table 2 presents the simulation of the hydrofoil ship at the various foil angles of attack (interval of 5 degrees), where the value of Froude number is set with the constant number of 1.545. In addition, the effect of Froude numbers into the total ship resistance characteristics are summarized in Table 3. In this case, the angles of attack for the fore and the aft foils are constant; whilst the Froude numbers have been run for the values of Fr = 1.382, 1.423, 1.545, 1.626, 1.708, and 1.830.

Table 2
Matrix of simulation with various foil angles of attack

Froude No.	Angle of Attack (°)							
	Fore Foil				Aft Foil			
1.545	0	5	10	15	0	5	10	15

Table 3
Matrix of simulation at various Froude number

Angle of Attack (°)		Froude Numbers					
Fore Foil	Aft Foil						
5	5	1.382	1.423	1.545	1.626	1.708	1.830

2.5 Computational Domain

In the boundary setting, the unstructured hexahedral meshes has been applied as shown in Figure 3. The ship's hydrostatic data such as mass, center of buoyancy, second moment of inertia and are obtained as the input data in the computational simulation. Here, the hydrofoil ship motion i.e., heave and pitch motions has been set as the solved. This means the hydrofoil ship is considered as the moving objects both of the vertical and the rotational motions during the computational simulation.

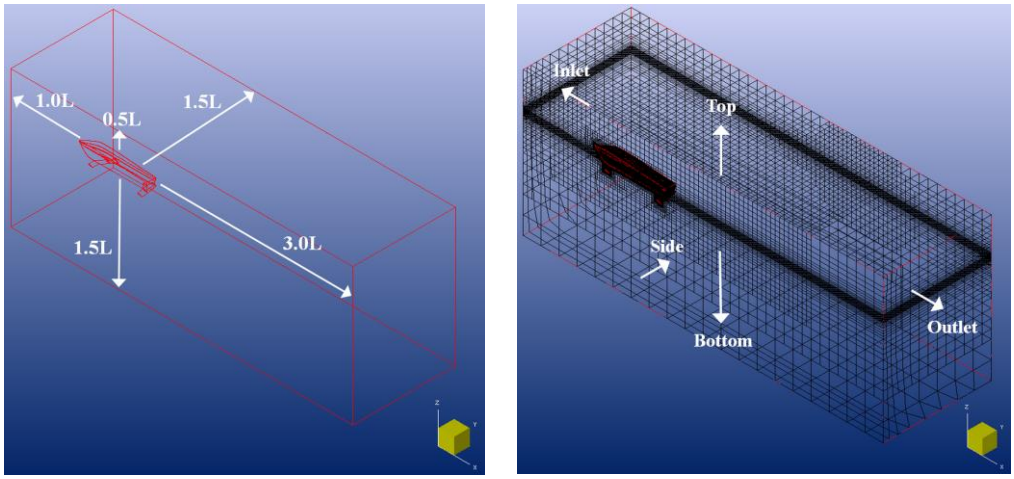

(a) Dimension of boundary setting (b) Meshing

Fig. 3. Boundary condition of hydrofoil model

2.6 Boundary Condition

The type of boundary conditions has been accordingly defined during in the initial stage of the computational domain. The definition of each boundary setting conditions and type of patches are clearly presented in Table 4. The example of the computational simulation result with respect to the total ship's resistance and lift force have been shown in Figure 4; and visualized using a package software called CFView^{TM} with respect to the wave elevation as displayed in Figure 5.

Table 4
Specific names and boundary type and condition of each patch of hydrofoil

Description	Type	Condition
Ymin	MIR	-
Zmax	EXT	Prescribed Pressure
Xmin	EXT	Far field
Ymax	EXT	Far field
Zmin	EXT	Prescribed Pressure
Xmax	EXT	Far field
Deck	SOL	Slip
Transom	SOL	Wall-function
Hull	SOL	Wall-function
Fore Strut	SOL	Wall-function
Fore Foil	SOL	Wall-function
Aft Strut	SOL	Wall-function
Aft Foil	SOL	Wall-function

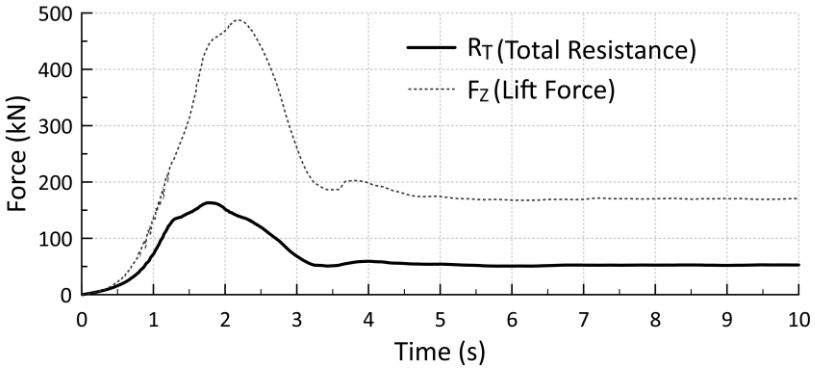

Fig. 4. Time-history of total ship's resistance and lift force of hydrofoil at Fr = 1.382

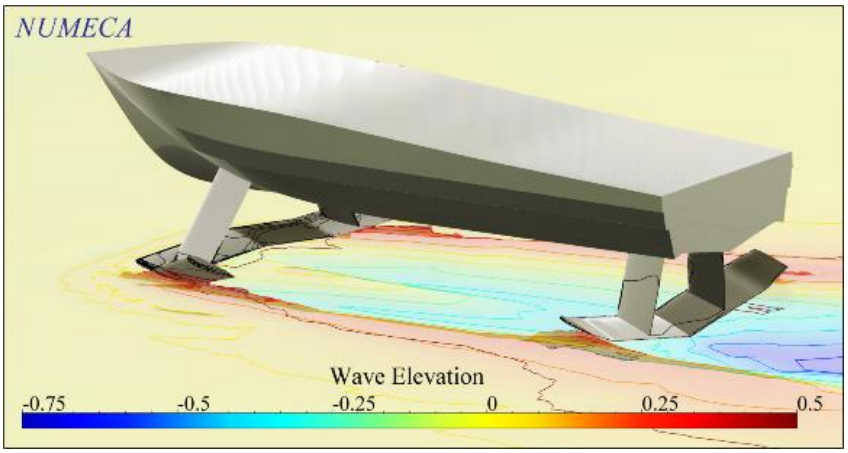

Fig. 5. 3D visualisation of wave elevation at Fr = 1.382

3. Results and Discussion

The CFD simulations have been successfully carried out to predict the total ship's resistance and the lift force on the hydrofoil in the calm water condition. The effects of various angles of attack and Froude numbers are accordingly discussed.

3.1 Lift Force Characteristics at Various Angles of Attack for Fore and Aft Foils

The prediction of the lift force (F_L) at the various angles of attack (AoA) on the fore and aft foils have been displayed in Figure 6. These various configurations have been independently evaluated in the calm water at the constant forward speed of Fr = 1.545. The results showed that the lift forces subsequently increase as the AoA for the fore foil increases from 0 degree up to 10 degrees. However, the lift force has decreased by 27% as the further increase of the AoA by 15 degrees as depicted in Figure 6(a). In addition to the aft foil, the lift force has gradually decreased commencing from the AoA of 5 degrees, where the further increase of the AoA up to 10 degrees caused the lift force reduced by 18%. These reductions of the lift forces of the fore and aft foils were proportional to the magnitude of the turbulent viscosities as well-visualized in Figure 7(d) and 8(c), respectively. The results of the lift forces and their lift forces coefficients are completely presented in Table 5 and Table 6. In general, the characteristics of the fore and aft foils at the various angles of attack included strong nonlinearities to induced their dynamic lift forces; whilst the fore foil has the higher lift forces at the AoA of 10 degrees as compared to the aft foil. The shape and larger wetted surface area of the foil could be the basic reason for the augmented the hydrodynamic forces, which is quantified in the form of the magnitude of the turbulent viscosity as accordingly depicted in Figure 7 and 8. Referring to the current simulation, the characteristics of the lift forces with respect to the various angles of attack are proportional to the value of their lift force coefficients (C_L).

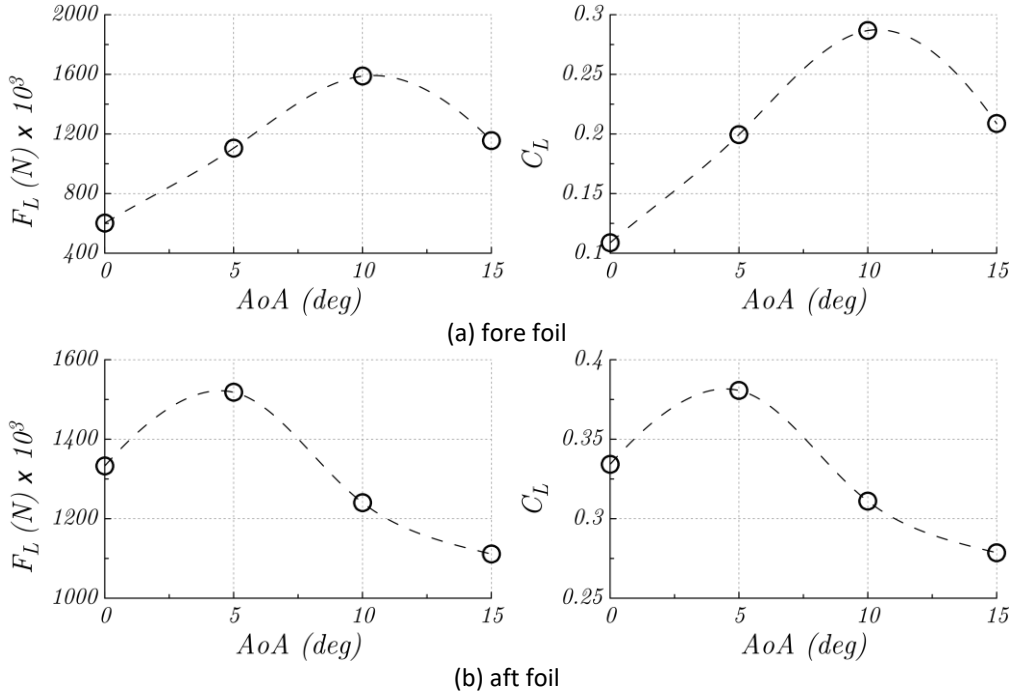

Fig. 6. Characteristics of lift force of fore and aft foils versus angles of attack

Table 5
Characteristics of the lift force at various angles of attack (fore foil)

Fore Foil's Angle of Attack (°)	F_L (N)	C_L
0	602.26236 x 10^3	0.10875
5	1104.72834 x 10^3	0.19948
10	1588.04863 x 10^3	0.28675
15	1155.85234 x 10^3	0.20871

Table 6
Characteristics of the lift force at various angles of attack (aft foil)

Aft Foil's Angle of Attack (°)	F_L (N)	C_L
0	1332.79600 x 10^3	0.33420
5	1518.00338 x 10^3	0.38064
10	1240.32375 x 10^3	0.31101
15	1111.09738 x 10^3	0.27861

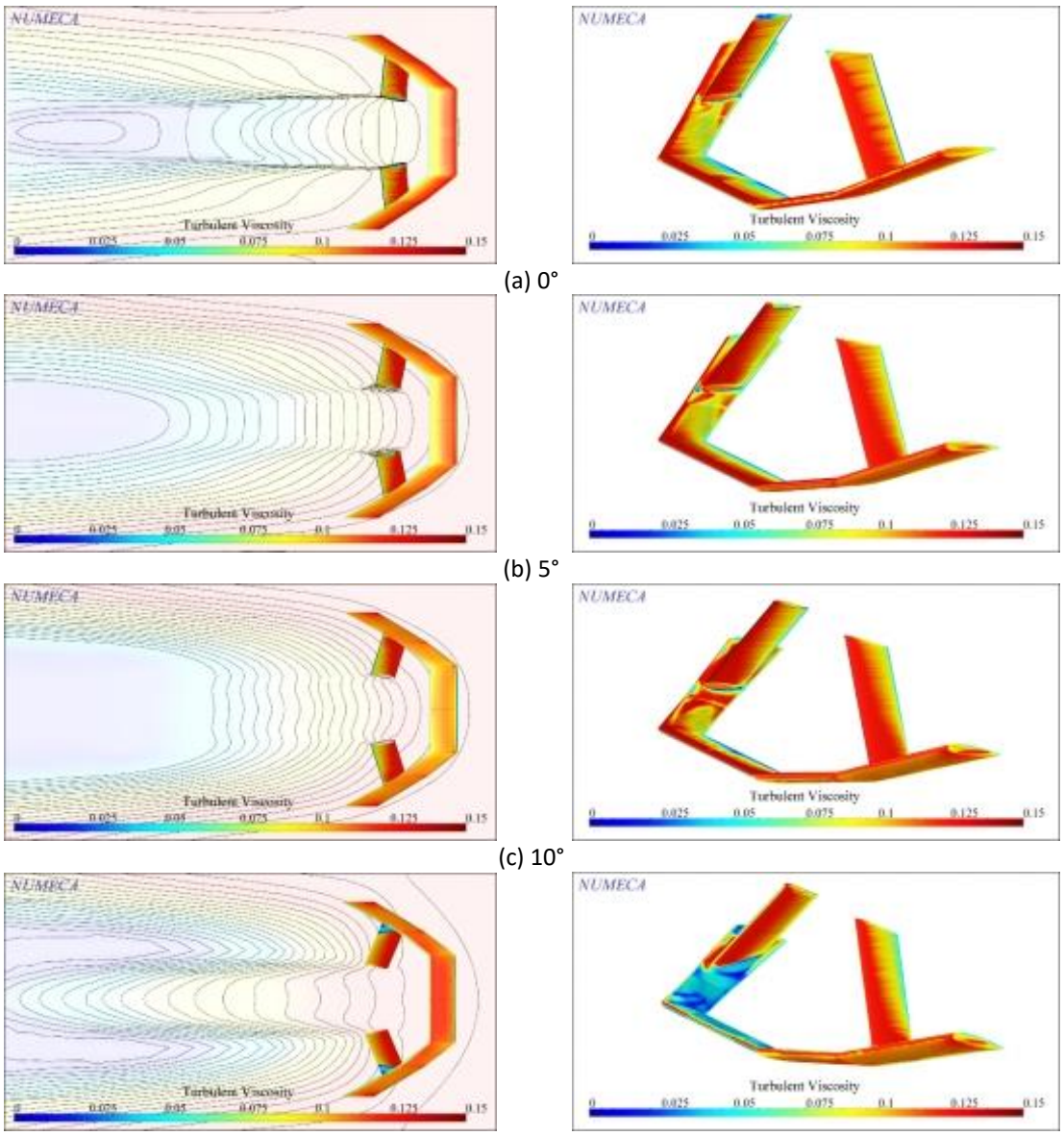

(a) 0°

(b) 5°

(c) 10°

(d) 15°

Fig. 7. Visualization of turbulent viscosity characteristics around fore foil at various angles of attack

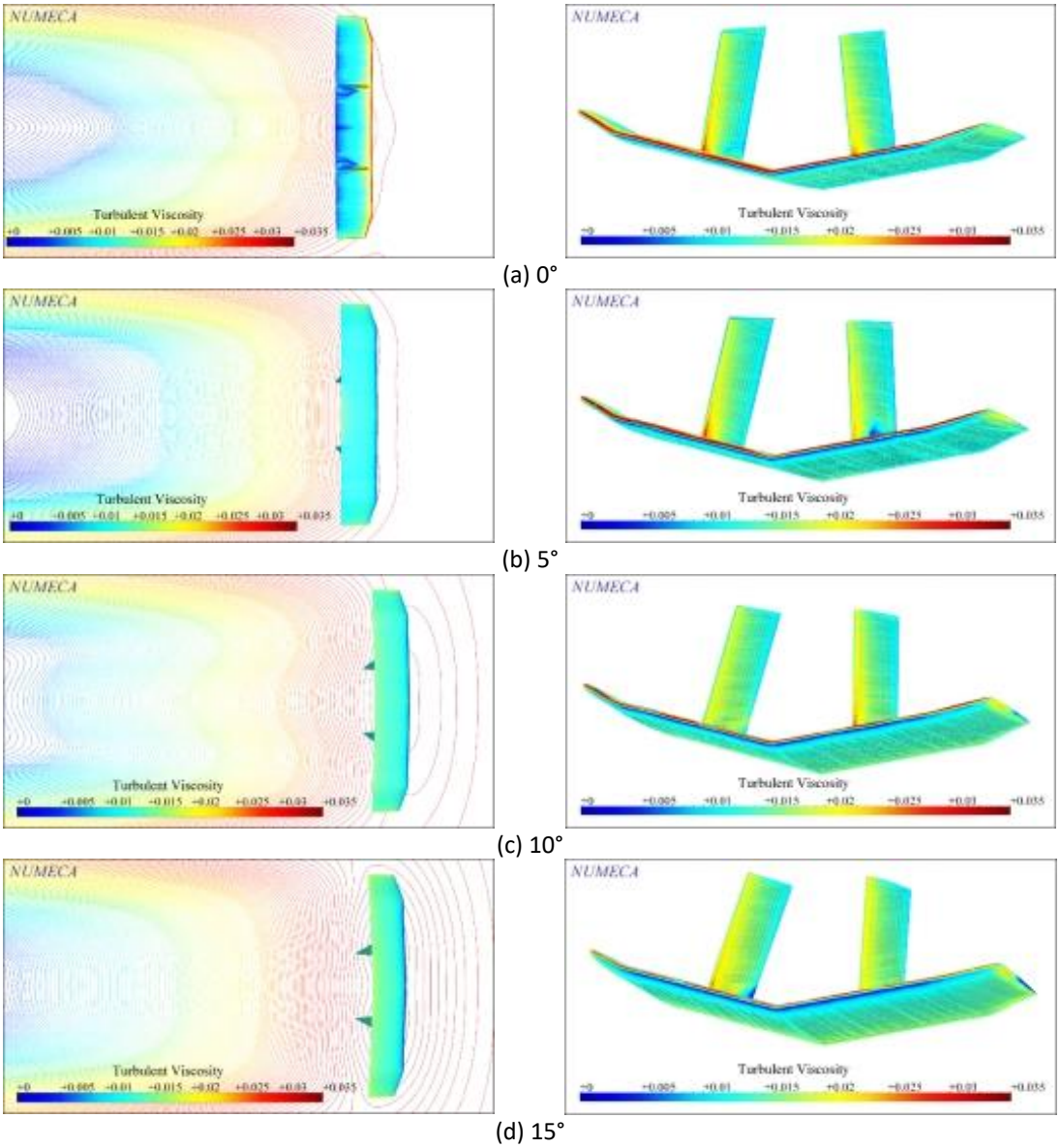

Fig. 8. Visualization of turbulent viscosity characteristics around aft foil at various angles of attack

3.2 Ship's Resistance Characteristics at Various Angles of Attack for Fore and Aft Foils

The characteristics of the total ship's resistance (R_T) of the hydrofoil at the various AoA are displayed in Figure 9. Similar to what was noted in Sub-sections 3.1, the value of Fr is constant, where the AoA is employed from 0 degree up to 15 degrees with the interval of 5°. The results revealed that the value of R_T is proportional with the value of AoA. In the case of the fore and aft foils, the increase of the AoA from 5 degrees to 10 degrees and 0 degree to 5 degrees resulted in the higher percentage of R_T increment by 120% and 102% as seen in Figure 9(a) and 9(b), respectively. The reason can be explained by the fact that the darker red color at the fore and aft foils surfaces in Figure 10(c) and 11(b) has significantly magnified the hydrodynamic pressure, which is proportional with the sufficient increase of the wave elevation as compared to Figure 10(b) and 11(a), respectively. The explanations can be comprehensively referred to Figure 10 and 11 for the better understanding in term of the hydrodynamic performances and wave elevations around the fore and aft foils. Regardless of the values of the angle of attacks as depicted in Figure 9(b), the aft foil showed the higher total ship's resistance as compared to the value of R_T for the fore foil.

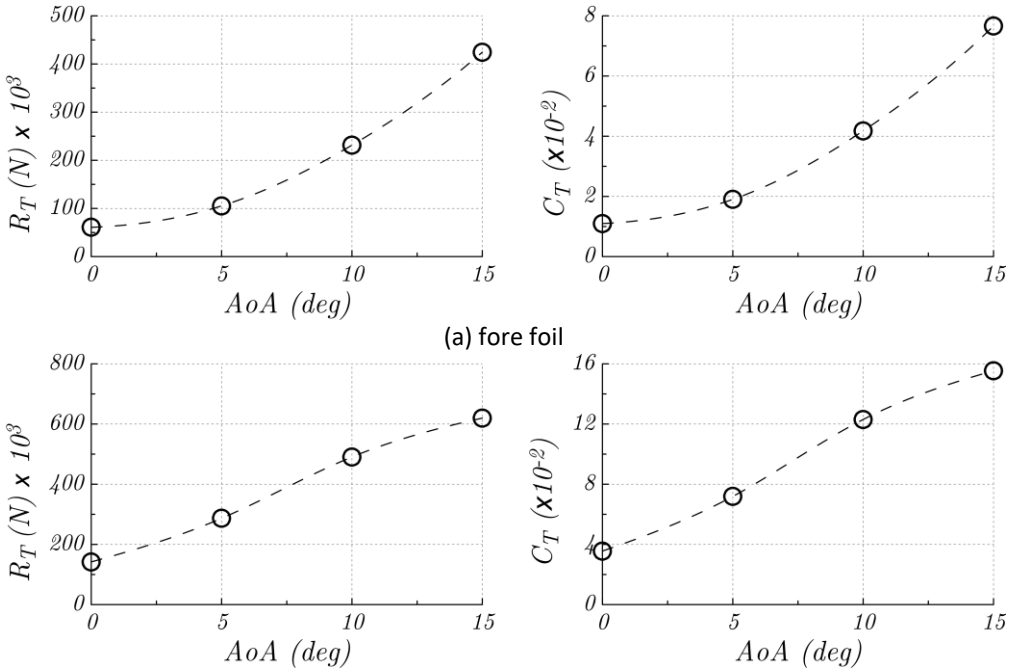

(a) fore foil

(b) aft foil

Fig. 9. Characteristics of total ship's resistance and aft foils at versus angles of attack

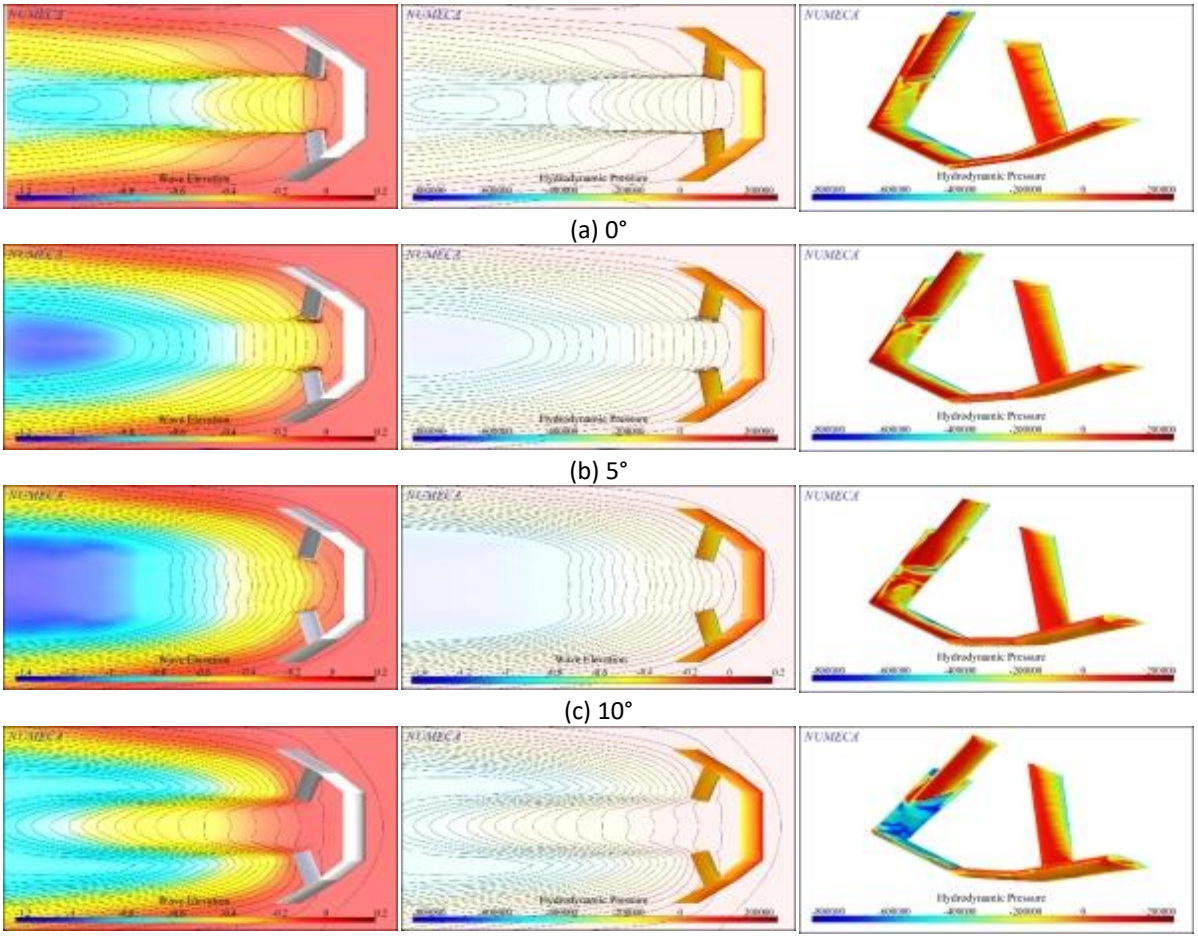

(a) 0°

(b) 5°

(c) 10°

(d) 15°

Fig. 10. Visualization of wave elevation (left) and hydrodynamic pressure (middle and right) around fore foil at various angles of attack

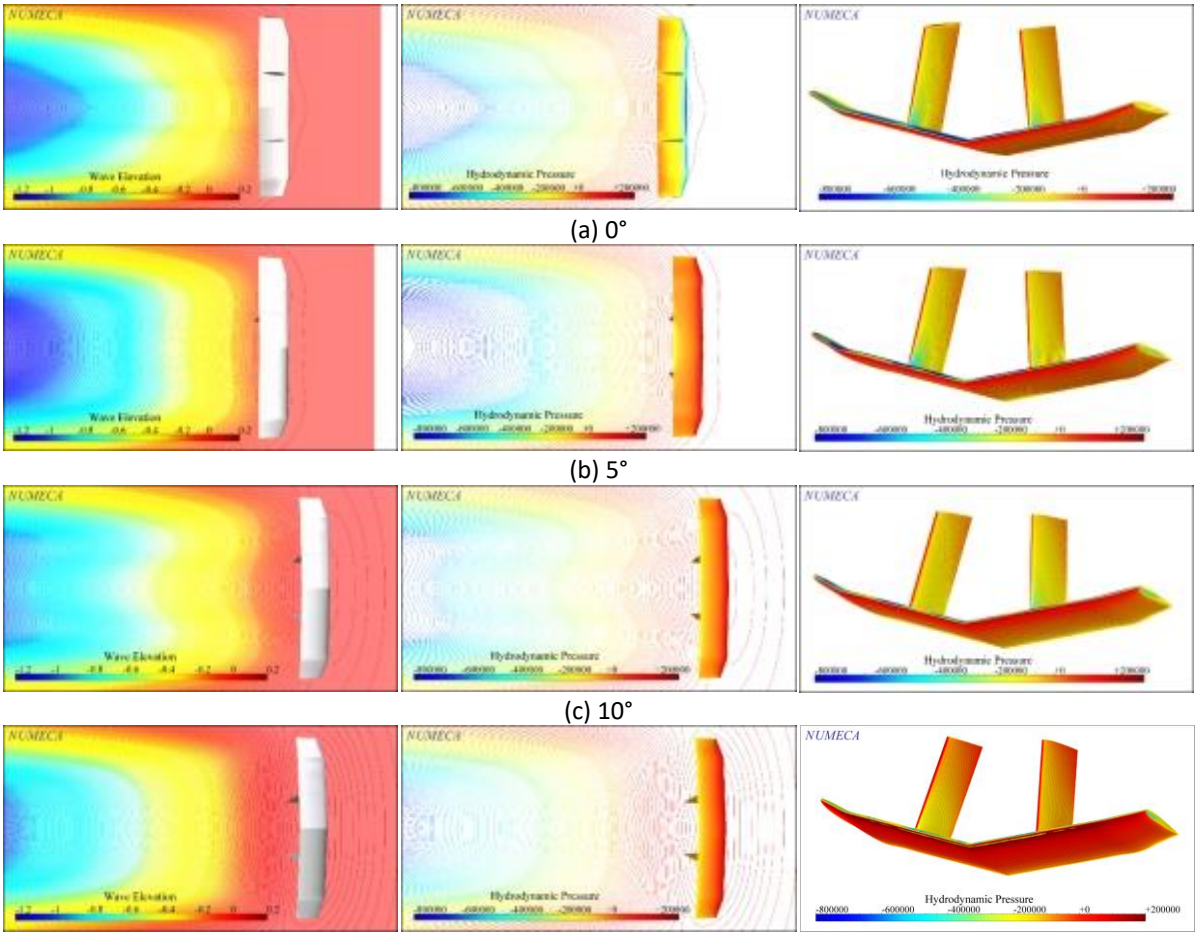

Fig. 11. Visualization of wave elevation (left) and hydrodynamic pressure (middle and right) around aft foil at various angles of attack

The detailed values of R_T and C_T are completely summarized in Table 7 and Table 8. A reason for this may rest with the higher value of the wetted surface area (WSA) of the foil as the main component affected the total ship's resistance. It should be noted here that the WSA value of the aft and fore foils are 29.029 m^2 and 20.904 m^2, respectively.

Table 7
The total ship's resistance at various angles of attack (fore foil)

AoA of Fore Foil (°)	R_T (N) x 10^3	C_T
0	60.867	0.01099
5	105.346	0.01902
10	231.451	0.04179
15	424.485	0.07665

Table 8
The total ship's resistance at various angles of attack (aft foil)

AoA of Aft Foil (°)	R_T (N) x 10^3	C_T
0	141.915	0.03559
5	286.791	0.07191
10	490.583	0.12301
15	619.644	0.15538

3.3 Lift Force Characteristics at Various Froude Number Incorporated with Fore and Aft Foils

The lift forces characteristics of the hydrofoil ship at various Froude numbers are displayed in Figure 12. Here, the computational simulations have applied the coupled foils (fore and aft foils), where the values of AoA for fore and aft foils are 5 degrees. The computational results revealed that the subsequent increase of the forward velocities from 17.478 m/s up to 19.549 m/s was inversely proportional with the lift forces of the hydrofoil. The reasoning for this result is that the viscous resistance especially at the fore foil has gradually reduced as visualized in Figure 13(a), (b) and (c), where the dark red color of the turbulent viscosity of the fore foil gradually disappeared. It should be noted here that the increase of the hydrodynamic pressure was insignificant regardless the increase of the forward velocities as seen in Figure 13 (right). This means that the hydrofoil ship has steadily moved forward with almost constant lift forces. Meanwhile, the further increase of the forward velocity by 20.574 m/s has arisen the lift force as seen in Figure 12(a). In general, the lift force coefficient has led to decrease as the forward velocity increases. The values of the lift forces and the lift force coefficients are presented in Table 9. Although the increase of Froude numbers within the range of $1.382 \leq Fr \leq 1.626$, this interference factor of the hydrodynamic pressure and the turbulent viscosity were insignificant to influence the lift forces of the hydrofoil ship.

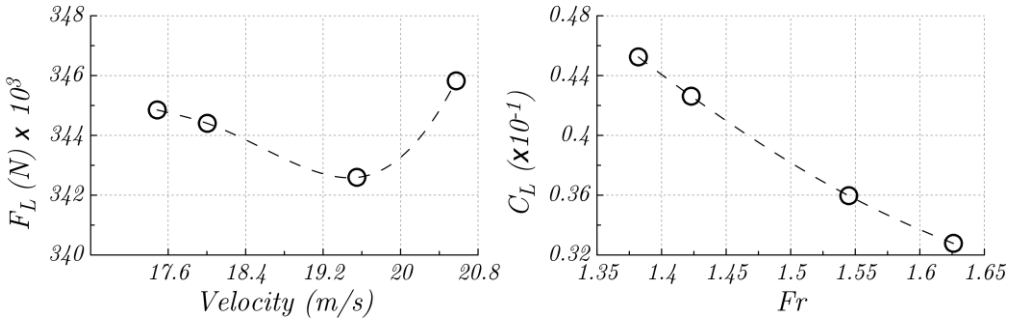

(a) F_L at fore foil = 5° and aft foil = 5° (b) C_L at fore foil = 5° and aft foil = 5°

Fig. 12. Lift force characteristics at various forward velocities

Table 9
Lift force characteristics of the hydrofoil ship at various Froude number

Froude No.	Velocity (m/s)	F_L (N) x 10^3	C_L
1.382	17.487	344.850	0.04524
1.423	18.005	344.399	0.04262
1.545	19.549	342.593	0.03596
1.626	20.574	345.824	0.03278

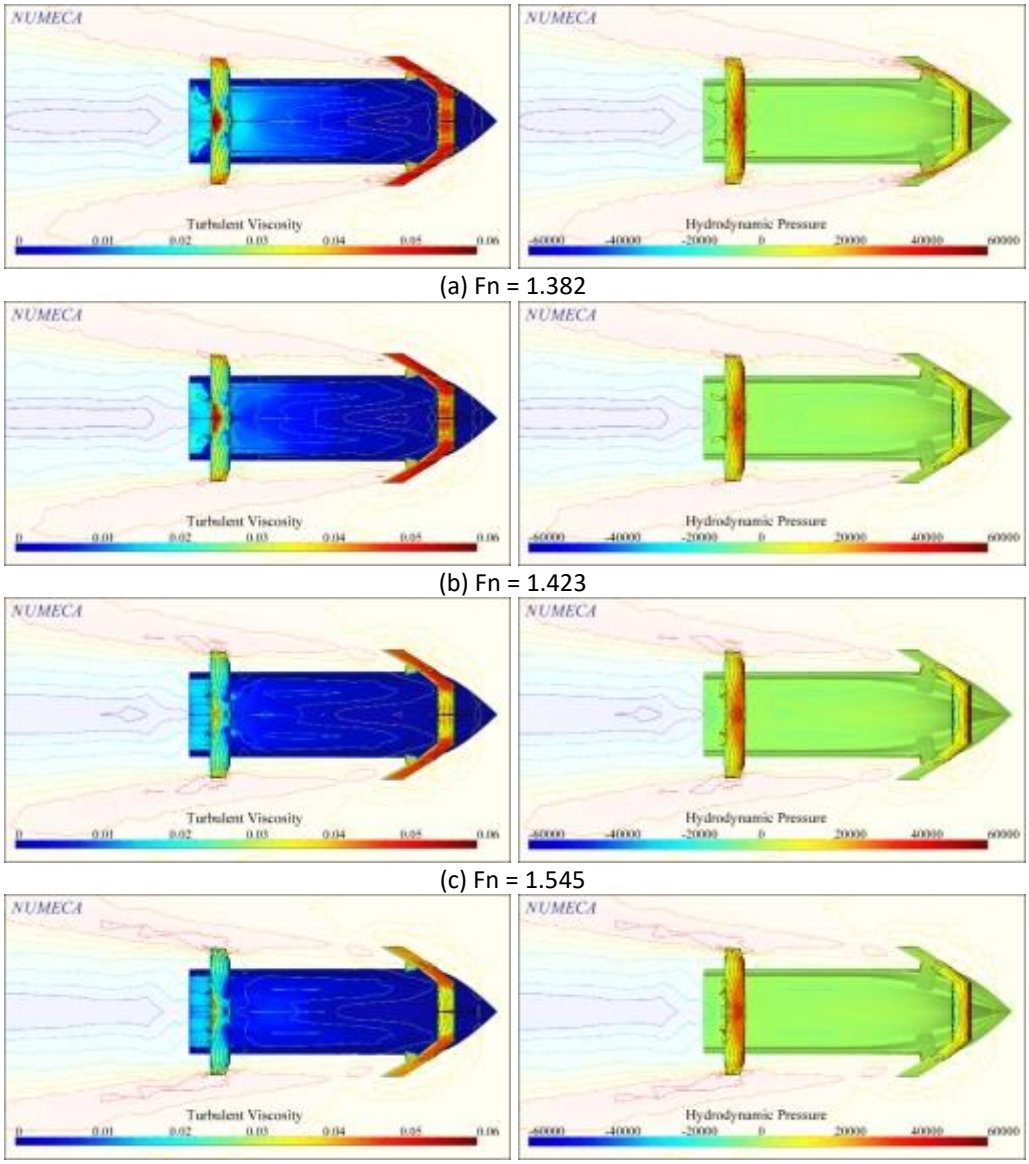

(a) Fn = 1.382

(b) Fn = 1.423

(c) Fn = 1.545

(d) Fn = 1.626

Fig. 13. Visualization of turbulent viscosity (left) and hydrodynamic pressure (right) around aft and fore foils at various Froude number

3.4 Resistance Characteristics at Various Froude Number Incorporated with Fore and Aft Foils

Figure 14 showed the characteristics of the total ship's resistance (R_T) with respect to the various forward velocities. Similar to what was noted in Sub-section 3.3, the subsequent increase of the forward velocities from 17.487 m/s up to 19.549 m/s was inversely proportional to the values of R_T. Referring to Figure 15(a), (b) and (c), this total resistance reduction occurred due to less magnitude of the wave elevation, which is proportional to the magnitude of the hydrodynamic pressure resistance. Correspondingly, it directly reduced the total ship's resistance coefficient (C_T) as seen in Figure 14(b). It can be merely concluded that the increase of Froude numbers from 1.382 up to 1.626 resulted insignificant effect to the total ship's resistance characteristics (Table 10).

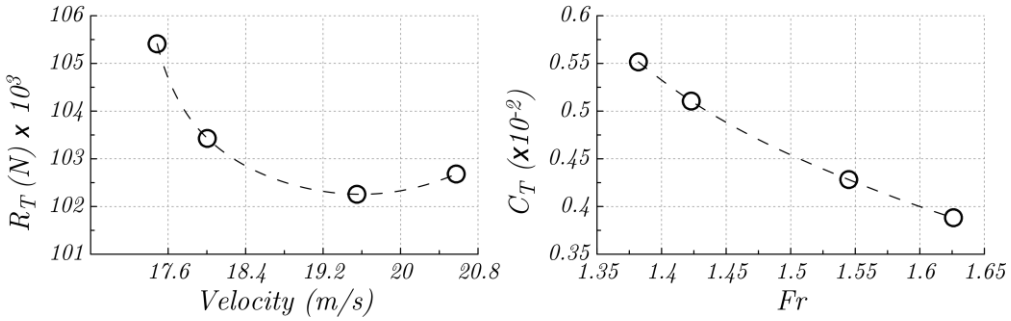

(a) R_T at fore foil = 5° and aft foil = 5° (b) C_T at fore foil = 5° and aft foil = 5°

Fig. 14. Resistance characteristics at various forward velocities

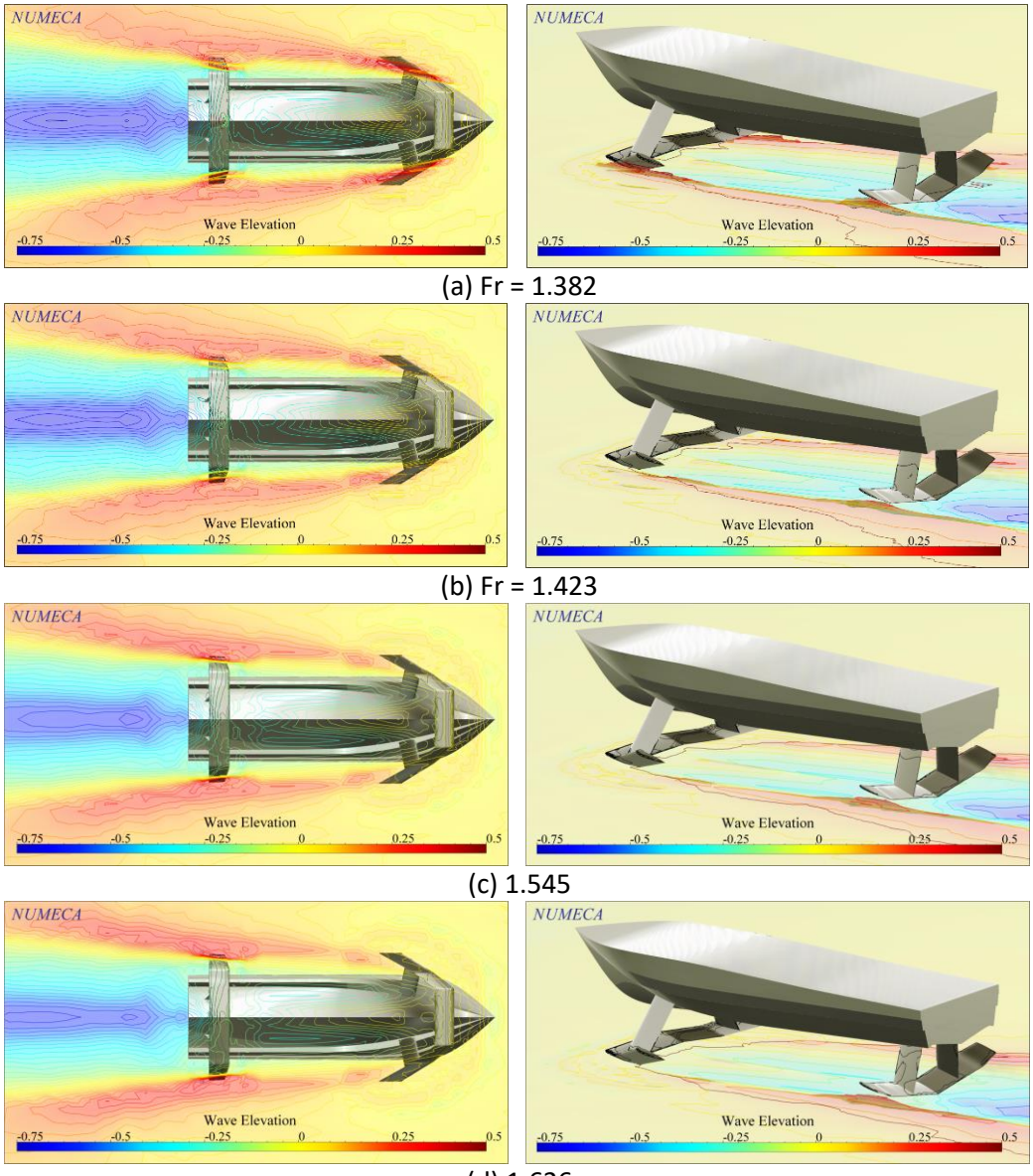

(a) Fr = 1.382

(b) Fr = 1.423

(c) 1.545

(d) 1.626

Fig. 15. Visualization of turbulent viscosity around aft (5°) and fore (5°) foils at various Froude numbers

Table 10
Resistance characteristics of the hydrofoil ship at various Froude number

Froude No.	Velocity (m/s)	R_T (N) x 10^3	C_T
1.382	17.487	105.411	0.01383
1.423	18.005	103.428	0.01279
1.545	19.549	102.257	0.01073
1.626	20.574	102.679	0.00973

4. Conclusion

The computational simulation on predicting the lift force and the total ship's resistance of the hydrofoil has successfully conducted. The effect of the angle of attack and Froude numbers have been taken into account. The results can be drawn as follows

i. The increase of the angle of attack for the fore foil from 5 degrees to 10 degrees resulted in the significant increase of the total ship's resistance by 120%.
ii. It should be noted that the lift force of the fore foil has decreased by 27% as the further increase of the angle of attack by 15 degrees.
iii. As compared to the effect of the angle of attacks, the subsequent increase of Froude numbers from 1.382 up to 1.626 has insignificant effect to the magnitude of the lift force and the total ship's resistance of the hydrofoil.

Acknowledgements
The authors wish to greatly thank Computer Simulation Laboratory, Department of Naval Architecture, Faculty of Ocean Engineering, Technology and Informatics, Universiti Malaysia Terengganu. This research was not funded by any grant.

References
[1] John, Bader. "Hydrofoils and retraction mechanism therefor." U.S. Patent 3,343,513, issued September 26, 1967.
[2] Matveev, K. I. "Tone generation on a hydrofoil of a high-speed ship." *Ocean engineering* 29, no. 10 (2002): 1283-1293. https://doi.org/10.1016/S0029-8018(01)00070-1
[3] Loveday, Howard. "The design of a hydrofoil system for sailing catamarans." PhD diss., Stellenbosch: University of Stellenbosch, 2006.
[4] Suastika, K. "Effects of stern-foil submerged elevation on the lift and drag of a hydrofoil craft." In *IOP Conference Series: Earth and Environmental Science*, vol. 135, no. 1, p. 012003. IOP Publishing, 2018. https://doi.org/10.1088/1755-1315/135/1/012003
[5] Putranto, Teguh, and Aries Sulisetyono. "Lift-drag coefficient and form factor analyses of hydrofoil due to the shape and angle of attack." *International Journal of Applied Engineering Research* 12, no. 21 (2017): 11152-11156.
[6] Djavareshkian, Mohammad Hassan, and Ali Esmaeili. "Heuristic optimization of submerged hydrofoil using ANFIS–PSO." *Ocean engineering* 92 (2014): 55-63. https://doi.org/10.1016/j.oceaneng.2014.09.033
[7] Besana, G. and Turnock S. R. "Computational Methods for Hydrofoil Design A composite analysis using panel code and RANS." University of Southampton, 2015.
[8] Eickmeier J., Dalanaj, M., Gray, J. and Koteki, M. "OCE Hydrofoil Development Team Spring/Summer 2006: Final Report, Volatilis." Florida Institute of Technology, 2006.
[9] Matveev, Konstantin, and Ralph Duncan. "Development of the tool for predicting hydrofoil system performance and simulating motion of hydrofoil-assisted boats." In *High Speed and High Performance Ship and Craft Symposium, Everett/WA: ASNE, USA*. 2005.
[10] Deshpande, Sujay, P. Sundsbø, and Subhashis Das. "Ship resistance analysis using CFD simulations in Flow-3D." *The International Journal of Multiphysics* 14, no. 3 (2020): 227-236. https://doi.org/10.21152/1750-9548.14.3.227
[11] Farkas, Andrea, Nastia Degiuli, and Ivana Martić. "Towards the prediction of the effect of biofilm on the ship resistance using CFD." *Ocean Engineering* 167 (2018): 169-186. https://doi.org/10.1016/j.oceaneng.2018.08.055

[12] Fitriadhy, A., N. Razali, and N. AqilahMansor. "Seakeeping performance of a rounded hull catamaran in waves using CFD approach." *Journal of Mechanical Engineering and Sciences* 11, no. 2 (2017): 2601-2614. https://doi.org/10.15282/jmes.11.2.2017.4.0238
[13] Fitriadhy, A., and N. Amira Adam. "Heave and pitch motions performance of a monotricat ship in head-seas." *International Journal of Automotive and Mechanical Engineering* 14 (2017): 4243-4258. https://doi.org/10.15282/ijame.14.2.2017.10.0339
[14] Copisarow, Maurice. "Marine fouling and its prevention." *Science* 101, no. 2625 (1945): 406-407. https://doi.org/10.1126/science.101.2625.406
[15] Wu, Cheng-sheng, De-cai Zhou, Lei Gao, and Quan-ming Miao. "CFD computation of ship motions and added resistance for a high speed trimaran in regular head waves." *International journal of naval architecture and ocean engineering* 3, no. 1 (2011): 105-110. https://doi.org/10.3744/JNAOE.2011.3.1.105
[16] Dumitru, D. "Numerical investigation of a two-degrees-of-freedom ship model for pitch-roll motion." In *IOP Conference Series: Materials Science and Engineering*, vol. 145, no. 8, p. 082007. IOP Publishing, 2016. https://doi.org/10.1088/1757-899X/145/8/082007
[17] Malathi, Ylemini, and Bgeeta Chandra Sekhar. "Design and Optimization of Hydrofoil using CFD and Structural Analysis." *International Journal of Scientific Engineering and Technology Research* 5, no. 44 (2016): 9107-9116.
[18] Fitriadhy, A., M. K. Aswad, N. Adlina Aldin, N. Aqilah Mansor, A. A. Bakar, and WB Wan Nik. "Computational fluid dynamics analysis on the course stability of a towed ship." *Journal of Mechanical Engineering and Sciences* 11, no. 3 (2017): 2919. https://doi.org/10.15282/jmes.11.3.2017.12.0263
[19] Fitriadhy, A., M. A. Faiz, and S. F. Abdullah. "Computational fluid dynamics analysis of cylindrical floating breakwater towards reduction of sediment transport." *J. Mech. Eng. Sci* 11, no. 4 (2017): 3072-3085. https://doi.org/10.15282/jmes.11.4.2017.10.0276
[20] Fitriadhy, A., and N. Amira Adam. "Heave and pitch motions performance of a monotricat ship in head-seas." *International Journal of Automotive and Mechanical Engineering* 14 (2017): 4243-4258. https://doi.org/10.15282/ijame.14.2.2017.10.0339
[21] Fitriadhy, Ahmad, Nur Adlina Aldin, and Nurul Aqilah Mansor. "CFD analysis on course stability of a towed ship incorporated with symmetrical bridle towline." *CFD Letters* 11, no. 12 (2019): 88-98.
[22] Fitriadhy, Ahmad, Nurul Aqilah Mansor, Nur Adlina Aldin, and Adi Maimun. "CFD analysis on course stability of an asymmetrical bridle towline model of a towed ship." *CFD Letters* 11, no. 12 (2019): 43-52.
[23] Sahoo, Prasanta K., Lawrence J. Doctors, and Luke Pretlove. "CFD prediction of the wave resistance of a catamaran with staggered demihulls." In *International Conference on Marine Hydrodynamics*, (2006).
[24] Fitriadhy, A., N. Razali, and N. AqilahMansor. "Seakeeping performance of a rounded hull catamaran in waves using CFD approach." *Journal of Mechanical Engineering and Sciences* 11, no. 2 (2017): 2601-2614. https://doi.org/10.15282/jmes.11.2.2017.4.0238
[25] Fitriadhy, A., S. A. Azmi, N. Aqilah Mansor, and N. Adlina Aldin. "Computational fluid dynamics investigation on total resistance coefficient of a high-speed" deep-V" catamaran in shallow water." *International Journal of Automotive & Mechanical Engineering* 14, no. 2 (2017). https://doi.org/10.15282/ijame.14.2.2017.18.0347